VTC 2022 Spring

Distance-Aware Precoding for Near-Field Capacity Improvement in XL-MIMO

Zidong Wu, Mingyao Cui, Zijian Zhang, and Linglong Dai

Department of Electronic Engineering

Tsinghua University

June, 2022

Outline

Key Performance Indicators (KPI) of 6G

- The involving from 5G to 6G will further fuse the digital worlds and real worlds
- To support emerging applications, KPIs in 6G should be much superior to those in 5G

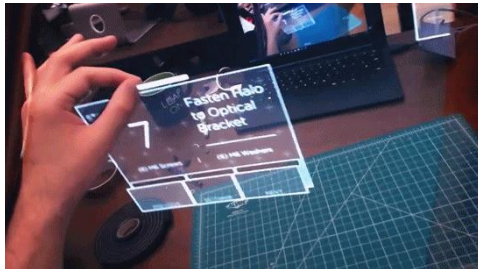

Extended Reality

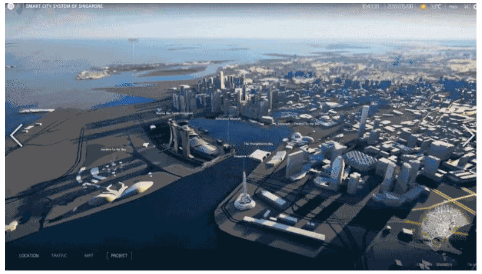

Digital Replica

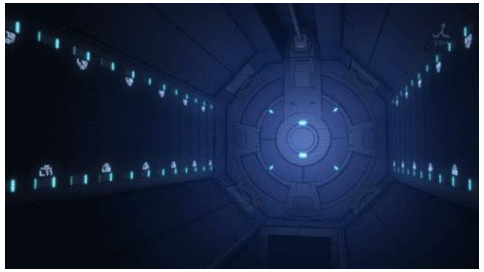

Holographic Video

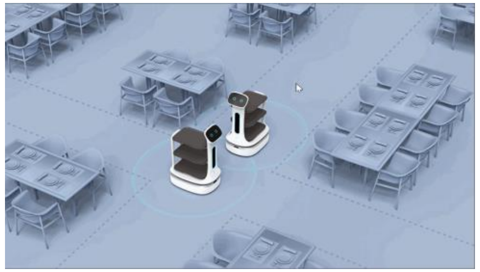

Intelligent Transport

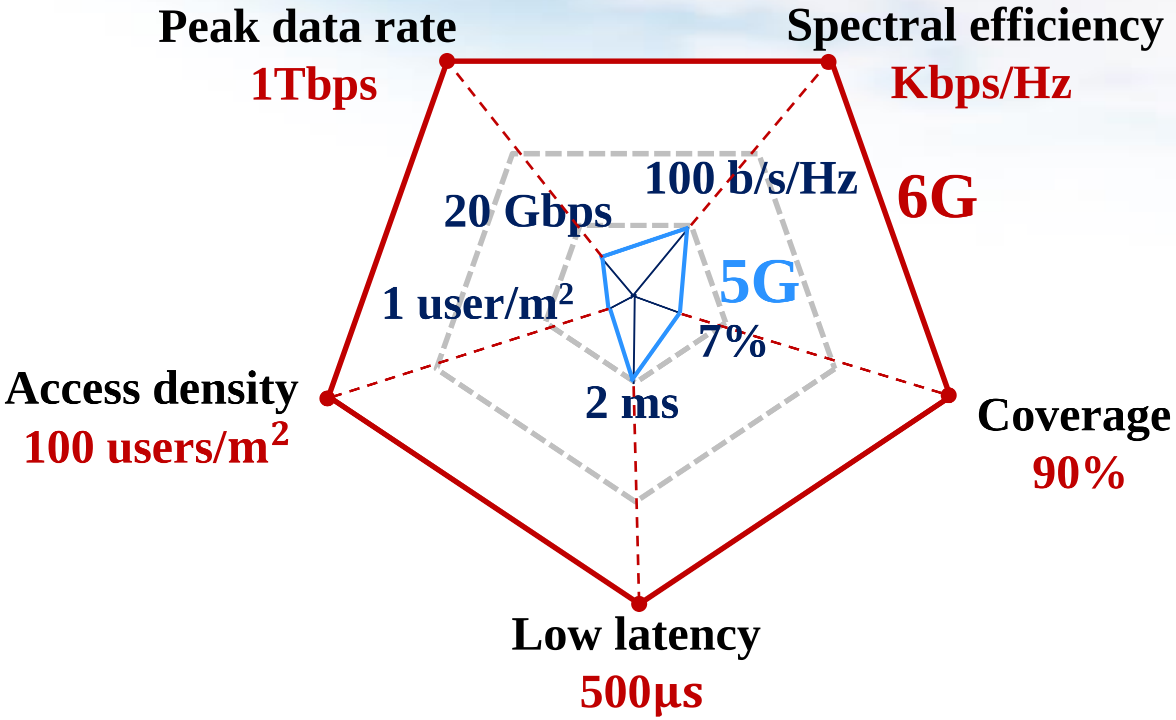

Spectral efficiency is expected to achieve 10 times increase

[1] ITU FG-NET-2030, "Network 2030-A Blueprint of Technology, Applications and Market Drivers towards the Year 2030 and Beyond," *https://www.itu.int/en/ITUT/ focusgroups/net2030/Documents/ White_Paper.pdf*, document ITU-T FG-NET-2030, ITU, Geneva, Switzerland, May 2019.

Extremely Large Antenna Arrays (ELAA)

- 6G is expected to achieve **10 times higher spectral efficiency** compared with 5G
- The higher spectral efficiency can be achieved exploiting **spatial multiplexing**, which requires significantly increased number of antennas
  - 4G: 2-8 antennas → 5G: 64-256 antennas
  - 6G: 1024+ antennas with **ultra-massive MIMO (UM-MIMO)** and **cell-free massive MIMO (CF-MIMO)**

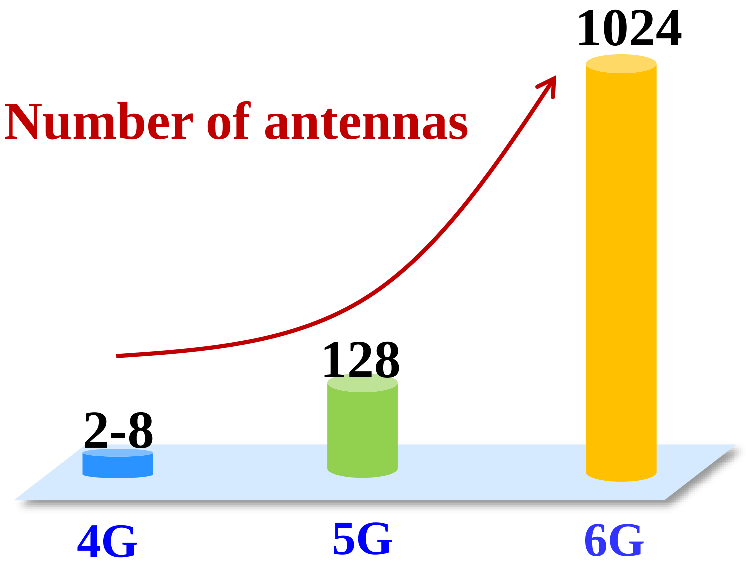

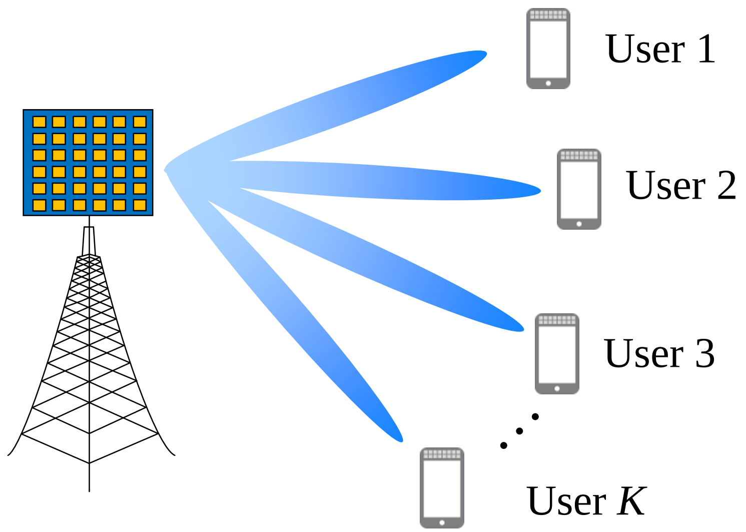

UM-MIMO

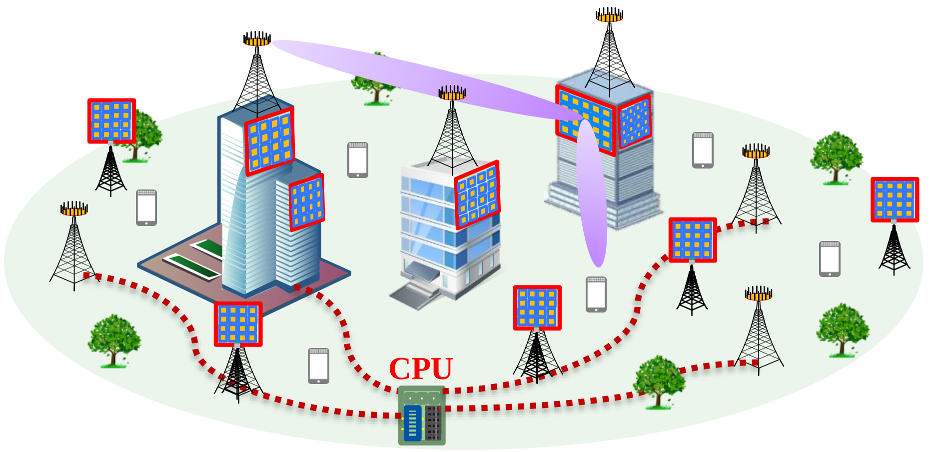

CF-MIMO

[1] W. Jiang, B. Han, M. A. Habibi and H. D. Schotten, "The Road Towards 6G: A Comprehensive Survey," *IEEE Open J. Commun. Soc.*, vol. 2, pp. 334-366, Feb. 2021.

EM Propagation: Near-field vs. Far-field

- **Electromagnetic (EM) propagation can be divided into far-field and near-field regions**
  - **Boundary of these regions is the Rayleigh distance**
  - **In far-field, EM propagation can be approximately modeled by the planar wave**
  - **In near-field, EM propagation has to be accurately modeled by the spherical wave**

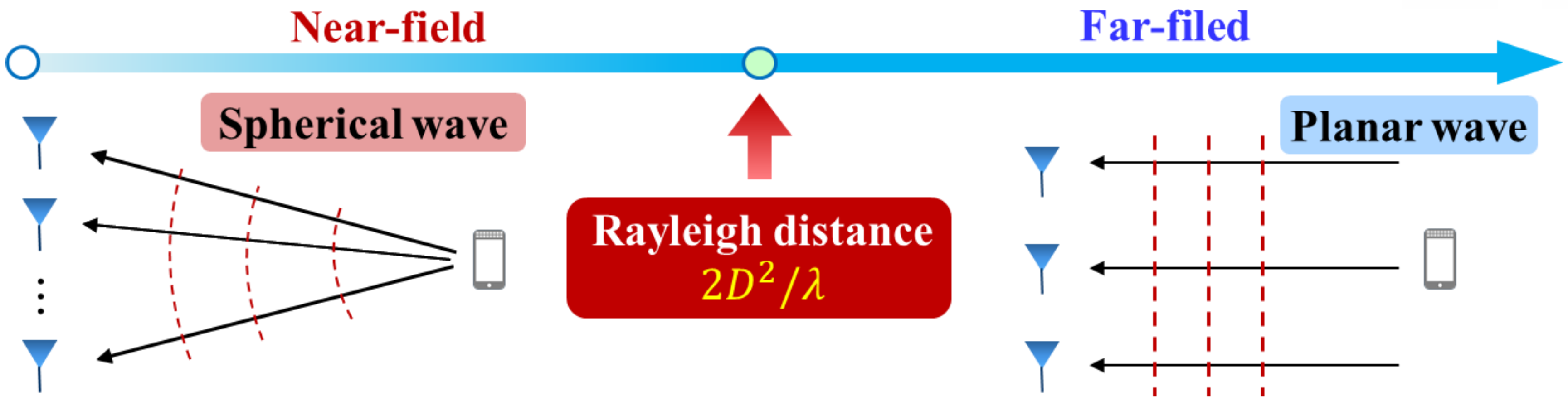

It has a critical difference of the EM characteristics between the near-field and far-field

[1] M. Cui, Z. Wu, Y. Lu, X. Wei, and L. Dai, "Near-field communications for 6G: Fundamentals, challenges, potentials, and future directions," *arXiv preprint arXiv:2203.16318*, Mar. 2022.

Challenges of Near-Field Communications

- **Challenges**
  - **Channel estimation**: near-field angle-domain channels suffer from a severe **energy spreading problem**
  - **Beam forming**: beamforming vectors are related to both **angles and distances**

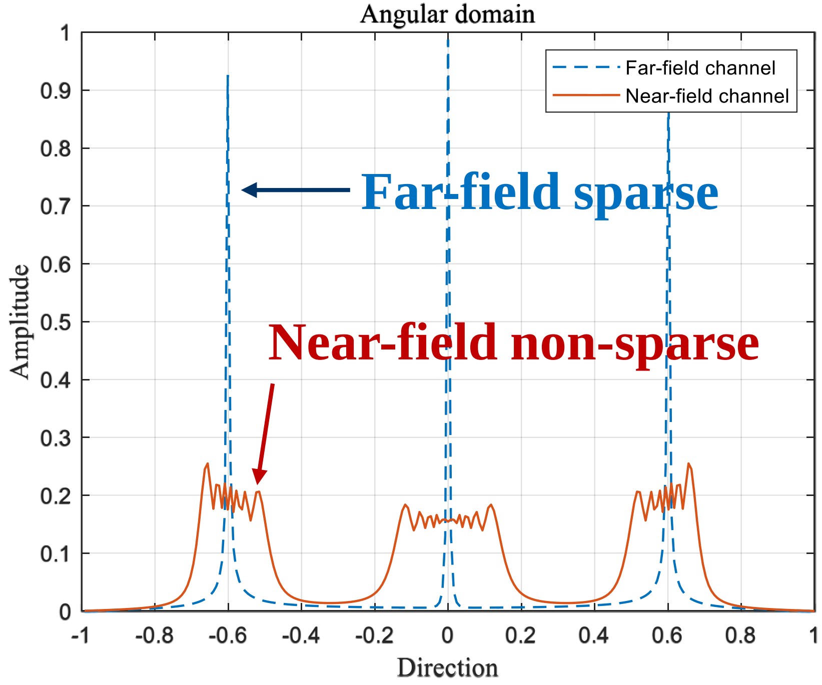

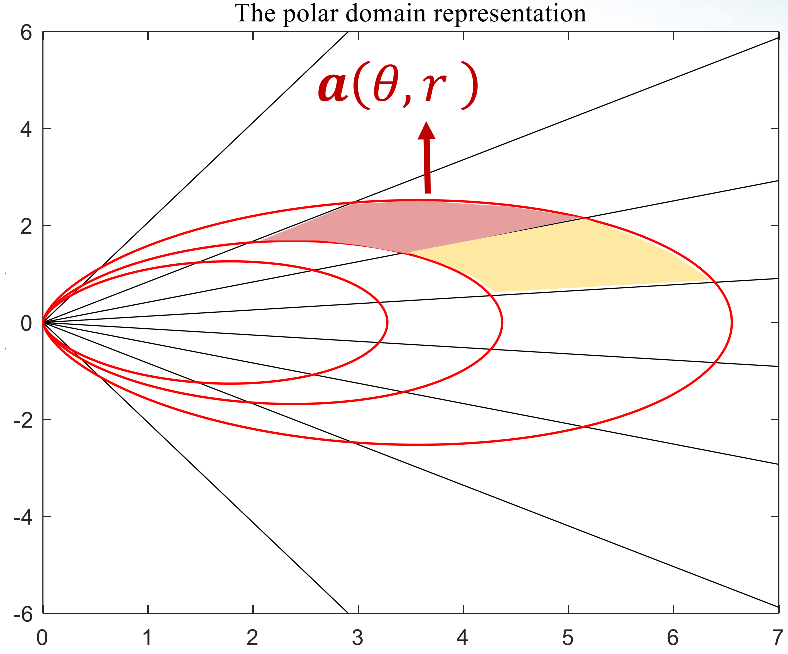

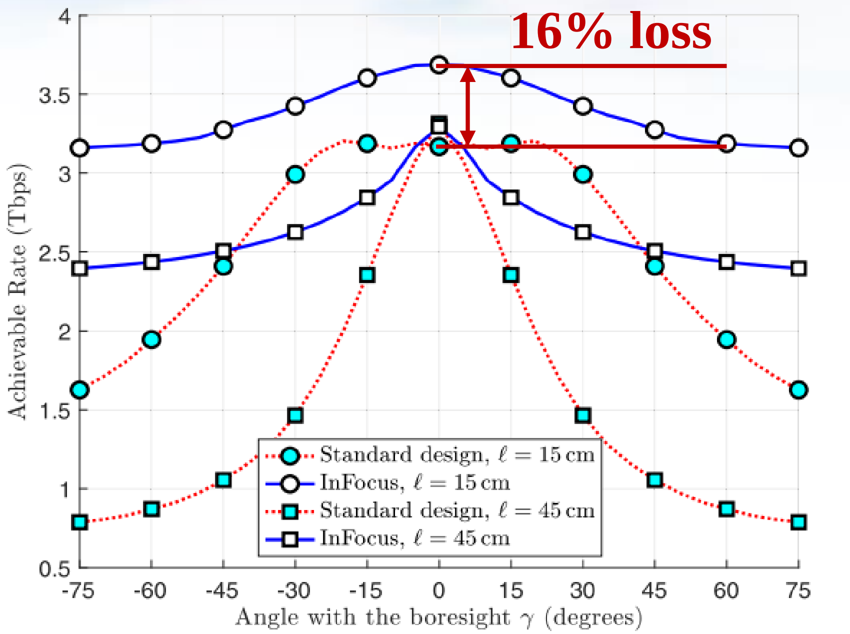

Overcoming near-field effect → Exploiting near-field effect

[1] M. Cui and L. Dai, "Channel estimation for extremely large-scale MIMO: Far-field or near-field?," *IEEE Trans. Commun.*, vol. 70, no. 4, pp. 2663-2677, Apr. 2022.

[2] N. J. Myers and R. W. Heath, "InFocus: a spatial coding technique to mitigate misfocus in near-field LoS beamforming," *IEEE Trans. Wireless Commun.*, vol. 21, pp. 2193-2209, April 2022.

Outline

Near-Field ELAA Communication System

- **System Model**
  - **Consider a single-user ELAA communication system with hybrid precoding**

$$\mathbf{y} = \mathbf{HFs} + \mathbf{n} = \mathbf{HF}_{\mathrm{A}}\mathbf{F}_{\mathrm{D}}\mathbf{s} + \mathbf{n}$$

Analog Precoder ($\mathbf{F}_{\mathrm{A}}$) **Digital Precoder** ($\mathbf{F}_{\mathrm{D}}$)

  - **Expression of sum rate** $$R = \max_{\mathbf{F},\ \mathbf{W}} \log_2 \left| \mathbf{I} + \frac{1}{\sigma_n^2} \mathbf{WHFF}^H \mathbf{H}^H \mathbf{W}^H \right|$$

Upper bound with digital $$R \le \sum_{i=1}^{\min(N_{\mathrm{t}}, N_{\mathrm{r}})} \log_2 \left(1 + \frac{p_i}{\sigma_n^2} \lambda_i^2(\mathbf{H}) \right)$$

i^{th} **singular value**

where $$p_i = \left(\frac{1}{\mu} - \frac{\sigma_{\mathrm{n}}^2}{\lambda_i^2(\mathbf{H})} \right)^+ \rightarrow 0(\lambda_i \rightarrow 0)$$

Capacity can be enhanced as the number of large singular values increases

Limited DoFs for Far-Field LoS Channel

- **Based on planar wave assumptions, degrees of freedom (DoF) are limited in line-of-sight (LoS) far-field channel**

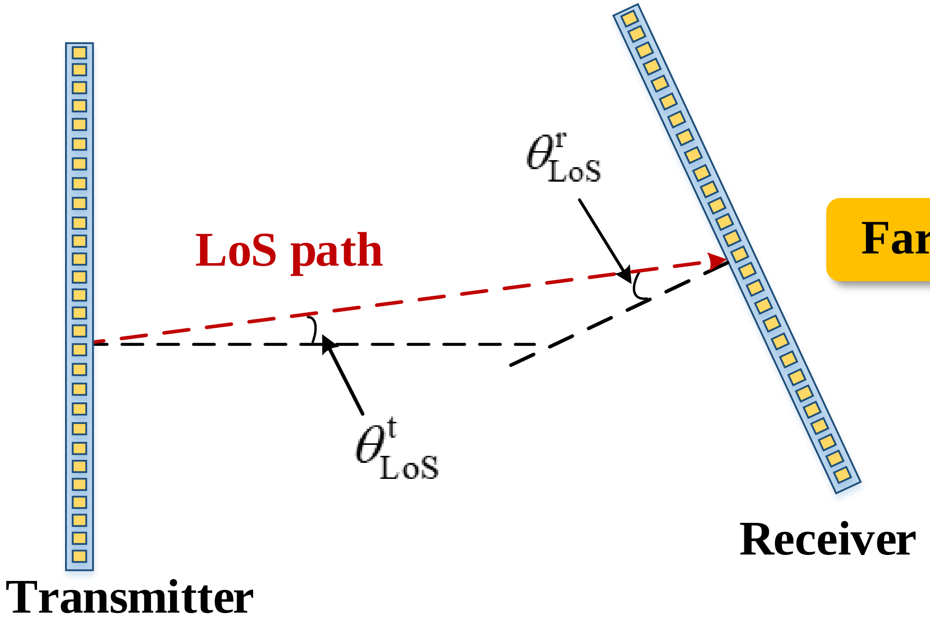

Far-field channel

Distance: $d^{(n)} = nd\theta$

Phase: $\phi_n^{\text{far}} = -\frac{2\pi d^{(n)}}{\lambda} = -\frac{2\pi}{\lambda} nd\theta$

Far-field steering vector

$$\mathbf{a}(\phi) = \frac{1}{\sqrt{N}}[1, e^{j\frac{2\pi}{\lambda}d\sin\phi}, \cdots, e^{j(2N)\frac{2\pi}{\lambda}d\sin\phi}]^T$$

$$\mathbf{H}_{\text{LoS}} = \alpha_{\text{LoS}} \underbrace{\mathbf{a}_{\text{r}}(\theta_{\text{LoS}}^{\text{r}})\, \mathbf{a}_{\text{t}}^H(\theta_{\text{LoS}}^{t})}_{\text{Rank-one matrix}}$$

The rank-one LoS channel can only support one data stream

[1] O. Ayach, S. Rajagopal, S. Abu-Surra, Z. Pi, and R. W. Heath, "Spatially sparse precoding in millimeter wave MIMO systems," *IEEE Trans. Wireless Commun.*, vol. 13, no. 3, pp. 1499–1513, Jan. 2014.

From Rank-one Channel to Highly-Ranked Channel

- **The rank-one far-field LoS channel is not valid any more in the near-field region**
- **Based on spherical waves, the near-field LoS channel becomes highly ranked**

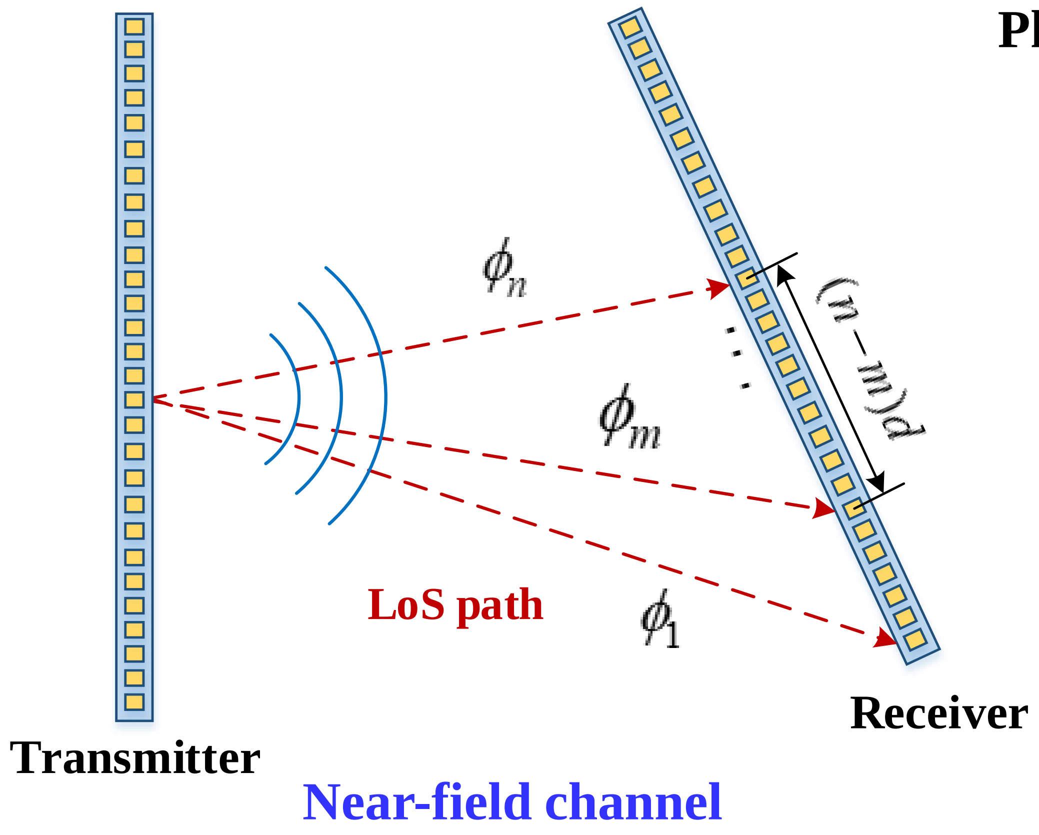

Phase: $\phi_n = \frac{2\pi(r^{(n)}-r)}{\lambda} = \frac{2\pi}{\lambda}\left(\sqrt{r^2 - 2ndr\theta + n^2d^2} - r\right)$

$$\overset{r > RD}{\approx} \underbrace{-\frac{2\pi}{\lambda} nd\theta}_{\text{Far-field phase } \phi_n^{\text{far}}}$$

❌ **Not valid in near-field region**

Far-field phase ϕ_n^{far}

⬇ **Near-field LoS channel**

$$\mathbf{H}_{\text{LoS}} = \underbrace{\begin{bmatrix} \alpha_{1,1} e^{-j2\pi r_{1,1}/\lambda} & \cdots & \alpha_{1,N_2} e^{-j2\pi r_{1,N_2}/\lambda} \\ \vdots & \ddots & \vdots \\ \frac{1}{r_{N_2,1}} e^{-j2\pi r_{N2,1}/\lambda} & \cdots & \frac{1}{r_{N_2,N_1}} e^{-j2\pi r_{N_2,N_1}/\lambda} \end{bmatrix}}_{\text{Significantly increased rank}}$$

Significantly increased rank

DoFs Analysis in the Near-Field Region

- **DoFs analysis of the near-field LoS channel**
  - ➢ **Inspired by the research of optics, the channel can be analyzed with continuous waves**

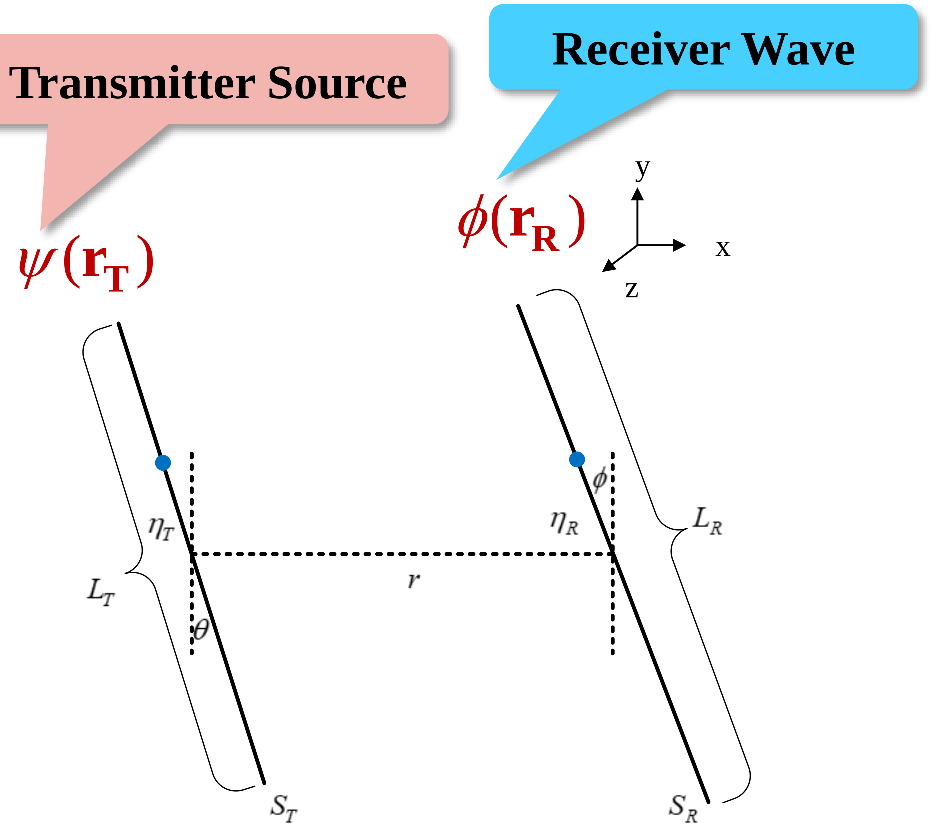

Continuous near-field LoS channel

$$\sigma^2 \mathbf{x} = \mathbf{H}^H \mathbf{H} \mathbf{x}$$

Eigenproblem

Sources in transmitter

$$\upsilon \psi(\mathbf{r_T}) = \int_{S_T} K(\mathbf{r_{T'}}, \mathbf{r_T}) \psi(\mathbf{r_{T'}}) d\mathbf{r_{T'}}$$

Convolution of Green Function

$$K(\mathbf{r_{T'}}, \mathbf{r_T}) = \int_{S_R} G^*(\mathbf{r_R}, \mathbf{r_{T'}}) G(\mathbf{r_R}, \mathbf{r_T}) d\mathbf{r_R}$$

Near-field Green function

$$G(\mathbf{r}, \mathbf{r}_1) = \frac{\exp(-jk|\mathbf{r} - \mathbf{r}_1|)}{4\pi |\mathbf{r} - \mathbf{r}_1|}$$

DoFs Analysis in the Near-Field Region

- **DoFs analysis of the near-field LoS channel**
  - **Inspired by the research of optics, the channel can be analyzed with continuous waves**

$$\upsilon\psi(\mathbf{r}_\mathbf{T}) = \int_{S_T} K(\mathbf{r}_{\mathbf{T}'},\mathbf{r}_\mathbf{T})\psi(\mathbf{r}_{\mathbf{T}'})d\mathbf{r}_{\mathbf{T}'}$$

$$= \int_{S_T}\int_{S_R} \frac{\exp(jk|\mathbf{r}_\mathbf{R}-\mathbf{r}_\mathbf{T}|)\exp(-jk|\mathbf{r}_\mathbf{R}-\mathbf{r}_{\mathbf{T}'}|)}{(4\pi)^2|\mathbf{r}_\mathbf{R}-\mathbf{r}_\mathbf{T}||\mathbf{r}_\mathbf{R}-\mathbf{r}_\mathbf{T}|} d\mathbf{r}_\mathbf{R}\psi(\mathbf{r}_{\mathbf{T}'})d\mathbf{r}_{\mathbf{T}'}$$

Near-field approximation $\sqrt{1+x} \approx 1 + \frac{1}{2}x - \frac{1}{8}x^2$

Singular values

prolate spheroidal wave function

Eigenproblem $$\upsilon_n\psi_n(c_y,\xi_T) = \int_{-1}^{1}\frac{\sin[c_y(\xi_T-\xi_{T'})]}{\pi(\xi_T-\xi_{T'})}\psi_n(c_y,\xi_{T'})d\xi_{T'}$$

Degrees of freedom $$N_{\mathrm{DoF}} \approx \frac{2}{\pi}c_y = \frac{D_t D_r\cos\theta\cos\phi}{\lambda r}$$

- **Proportion to aperture**
- **Inversely proportion to distance**

Increased DoFs for Near-Field LoS Channel

- **DoFs analysis of the near-field LoS channel**
  - **Accurate estimation of singular values with PSWFs**

$$\upsilon_n \psi_n(c_y, \xi_T) = \int_{-1}^{1} \frac{\sin[c_y(\xi_T - \xi_{T'})]}{\pi(\xi_T - \xi_{T'})} \psi_n(c_y, \xi_{T'}) d\xi_{T'}$$

- **Simulation**
  - Parallel positioned
  - Large-scale fading is neglected
  - $f = 30\ \text{GHz}$
  - $N_\text{t} = N_\text{r} = 256$
  - $d = \lambda / 2 = 5\ mm$

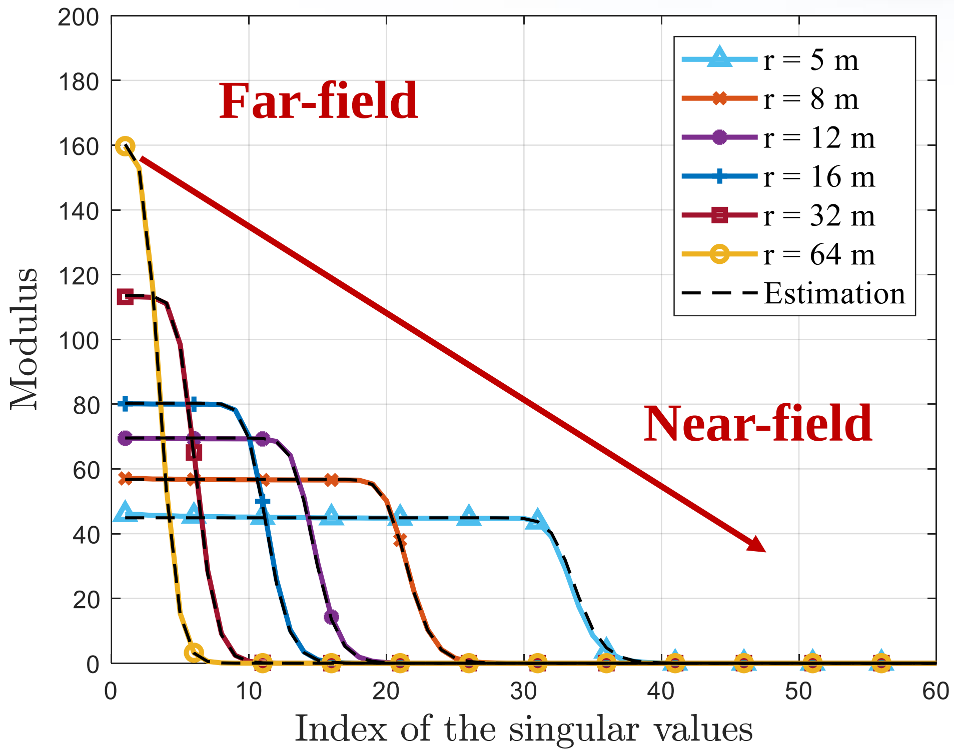

Limitation of hybrid precoding architecture

- However, limited by the small number of RF chains, the classical hybrid precoding can not efficiently utilize the increased DoFs to enhance the capacity

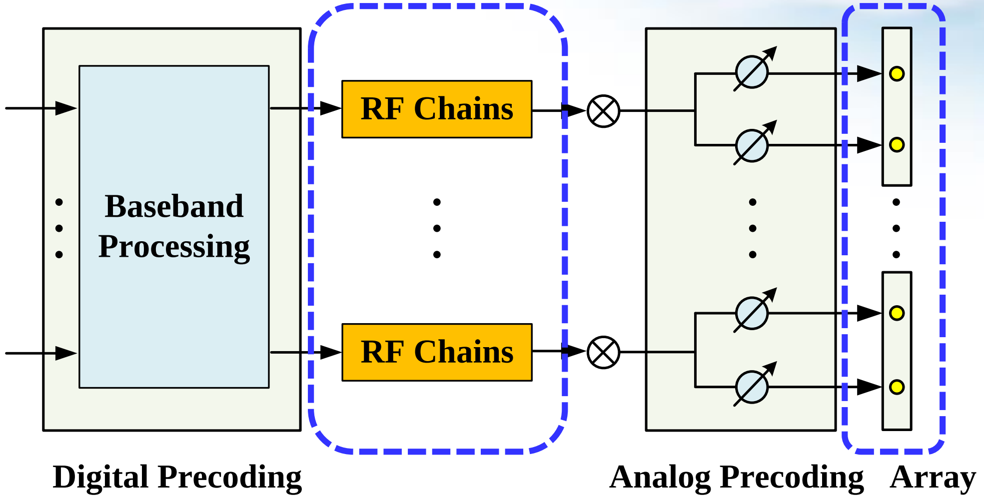

Precoding	Region	Spatial DoFs	RF chains	Spectral Efficiency
Hybrid Precoding	Far-Field	Low	RF Chains ≈ DoFs	Near Optimal
	Near-Field	High	RF Chains ≪ Distance-Related DoFs	Far From Optimal

How to efficiently utilize the significantly increased DoFs in near field

Outline

Distance-Aware Precoding Architecture

- Based on the **distance-related DoFs** in the near-field region, the distance-aware precoding architecture is proposed
- The number of **activated RF chains** can be configured to **match the increased DoFs** in the near-field region

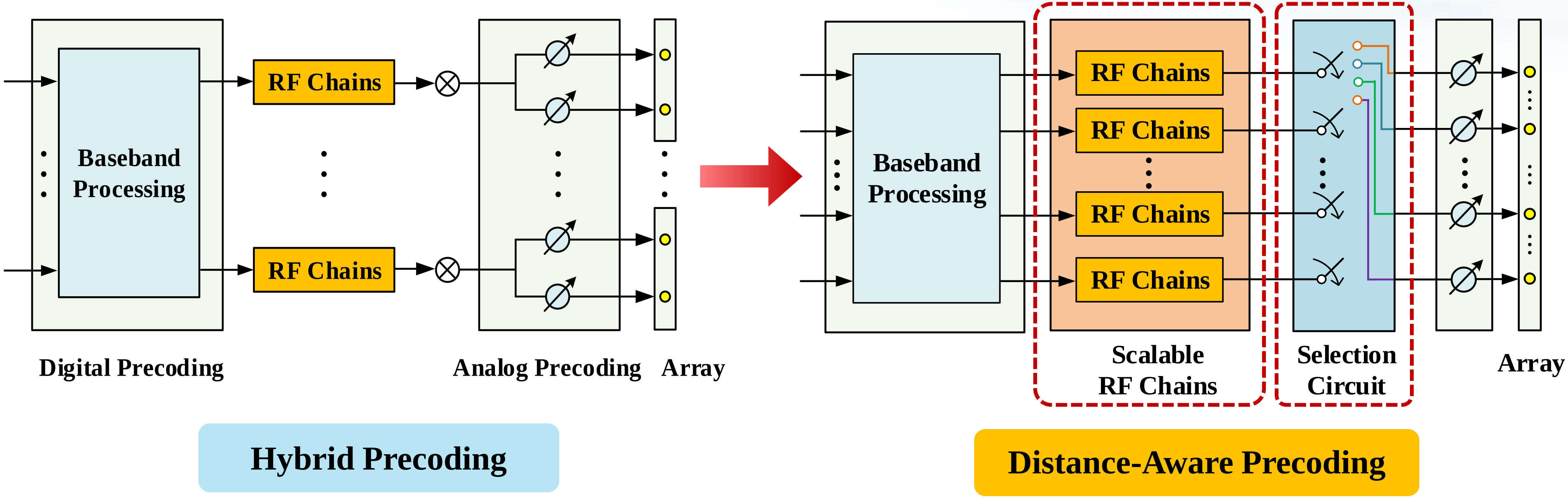

Distance-Aware Precoding Algorithm

- **Spectral efficiency maximization problem**

Selection Matrix

$$\max_{\mathbf{F}_{\mathrm{A}},\mathbf{F}_{\mathrm{S}},\mathbf{F}_{\mathrm{D}}} \left\{ R = \log_2\left(\left|\mathbf{I} + \frac{1}{\sigma_{\mathrm{n}}^2}\mathbf{H}\mathbf{F}_{\mathrm{A}}\mathbf{F}_{\mathrm{S}}\mathbf{F}_{\mathrm{D}}\mathbf{F}_{\mathrm{D}}^H\mathbf{F}_{\mathrm{S}}^H\mathbf{F}_{\mathrm{A}}^H\mathbf{H}^H\right|\right)\right\}$$

Analog Precoder | Digital Precoder

$$\text{s.t.}\ \ C_1 : \|\mathbf{F}_{\mathrm{A}}\mathbf{F}_{\mathrm{S}}\mathbf{F}_{\mathrm{D}}\|_F^2 \le P_{\mathrm{tot}}$$

$$C_2 : \mathbf{F}_{\mathrm{A}} \in F$$

$$C_3 : (\mathbf{F}_{\mathrm{S}})_{ij} \in \{0,1\}, \forall i, j$$

$$C_4 : \mathrm{diag}(\mathbf{F}_{\mathrm{S}}\mathbf{F}_{\mathrm{S}}^H) = \mathbf{1}_{N_t}$$

- **Optimization Process**
  - **Stage 1: Determine the optimal number of RF chains N_{S}**
  - **Stage 2: Determine the selection matrix $\mathbf{F}_{\mathrm{S}}$**
  - **Stage 3: Obtain the analog precoder $\mathbf{F}_{\mathrm{A}}$ and digital precoder $\mathbf{F}_{\mathrm{D}}$**

Distance-Aware Precoding Algorithm

- **Stage 1: Optimization of RF chains N_s**
  - **Similar to the classical hybrid precoding scheme, the purpose is to design the number of RF chains to match the valid spatial DoFs**

$$N_\mathrm{s}^{\mathrm{opt}} = \#\{p_i \mid p_i > 0\}$$

- **Stage 2: Optimization of selection matrix $\mathbf{F}_\mathrm{S}$**

$$R = \log_2\left(\left|\mathbf{I} + \frac{1}{\sigma_\mathrm{n}^2}\mathbf{H}\mathbf{F}_\mathrm{A}\mathbf{F}_\mathrm{S}\mathbf{F}_\mathrm{D}\mathbf{F}_\mathrm{D}^H\mathbf{F}_\mathrm{S}^H\mathbf{F}_\mathrm{A}^H\mathbf{H}^H\right|\right)$$

$$R = \sum_{i=1}^{N_\mathrm{s}}\log_2\left(1 + \frac{\lambda_i^2(\mathbf{H}\mathbf{F}_\mathrm{A}\mathbf{F}_\mathrm{S})p_i}{\sigma_\mathrm{n}^2}\right)$$

$$\leq N_\mathrm{s}\log_2\left(1 + \frac{1}{N_\mathrm{s}}\sum_{i=1}^{N_\mathrm{s}}\frac{\lambda_i^2(\mathbf{H}\mathbf{F}_\mathrm{A}\mathbf{F}_\mathrm{S})p_i}{\sigma_\mathrm{n}^2}\right)$$

$$\max_{\mathbf{F}_\mathrm{A},\mathbf{F}_\mathrm{S}}\sum_{i=1}^{N_\mathrm{s}}\lambda_i^2(\mathbf{H}\mathbf{P}_\mathrm{S}\mathbf{F}_\mathrm{A}\mathbf{F}_\mathrm{S}) \approx \sum_{i=1}^{N_\mathrm{s}}\lambda_1(\mathbf{H}_{\mathcal{S}_i}^H\mathbf{H}_{\mathcal{S}_i})$$

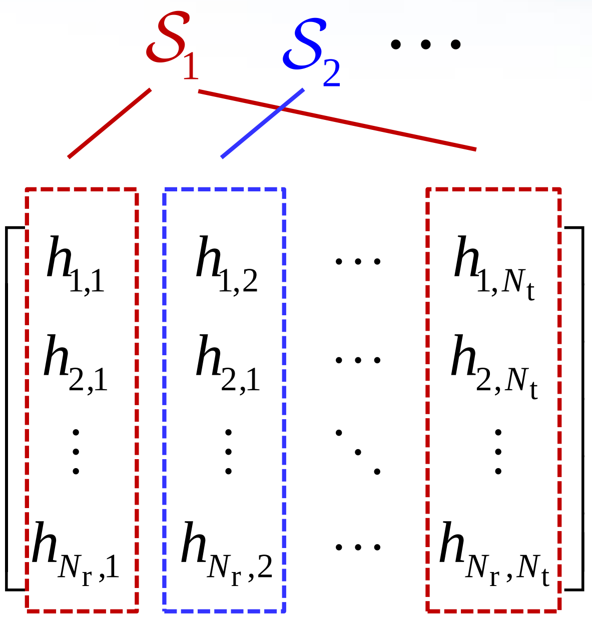

Classify the channel by column and maximize the sum of largest singular value

Distance-Aware Precoding Algorithm

- **Summary of the proposed optimization process for F_S**
  - **To optimize the selection matrix F_S, it is equivalent to partition the subarrays which maximizes the sum of the largest singular values**

Algorithm 2 Near-Field Subarray Partitioning Alogorithm.

Input: Channel $\mathbf{H}$, N_s, N_{bound} and N_t.

Output: $\mathcal{S}_1, \mathcal{S}_2, \cdots, \mathcal{S}_{N_s}$

$\mathbf{R} = \mathbf{H}^H\mathbf{H}$, $\mathcal{S}_{\text{sel}} = \varnothing$, $n_{\text{group}} = \lfloor \frac{N_t}{N_s} \rfloor$

Initialize $\mathcal{S}_i = \{i \cdot n_{\text{group}}\}$, $\mathcal{S}_{\text{sel}} \leftarrow \mathcal{S}_{\text{sel}} \cup \{i \cdot n_{\text{group}}\}$, for $i = 1, 2, \cdots, N_s$

for $k = 1 : N_t - N_s$ **do**

  $\{i_k, j_k\} = \underset{i\in\mathcal{S}_{\text{sel}}, j\notin\mathcal{S}_{\text{sel}}}{\text{argmax}} |[\mathbf{R}]_{i,j}|$

  $\hat{r} = \underset{r\in\{1,\cdots,N_s\}}{\text{argmax}} \hat{\lambda}_1(\mathbf{R}, \mathcal{S}_r \cup \{j_k\}) - \hat{\lambda}_1(\mathbf{R}, \mathcal{S}_r)$

  $\mathcal{S}_{\text{sel}} \leftarrow \mathcal{S}_{\text{sel}} \cup j_k$, $\mathcal{S}_{\hat{r}} \leftarrow \mathcal{S}_{\hat{r}} \cup j_k$

  if $|\mathcal{S}_{\hat{r}}| \geq N_{\text{bound}}$ **then**

    $\hat{m} = \underset{m\in\mathcal{S}_{\hat{r}}}{\text{argmin}} \sum_{n\in\mathcal{S}_{\hat{r}}} |\mathbf{R}_{m,n}|$

    $\hat{r}' = \underset{r'\neq\hat{r}}{\text{argmax}} \hat{\lambda}_1(\mathbf{R}, \mathcal{S}_{r'} \cup \hat{m}) - \hat{\lambda}_1(\mathbf{R}, \mathcal{S}_{r'})$

    $\mathcal{S}_{\hat{r}} \leftarrow \mathcal{S}_{\hat{r}} \backslash \hat{m}$, $\mathcal{S}_{\hat{r}'} \leftarrow \mathcal{S}_{\hat{r}'} \cup \hat{m}$

  end if

end for

for $l = 1 : N_s$ **do**

  $\hat{m} = \underset{m\in\mathcal{S}_l}{\text{argmin}} \sum_{n\in\mathcal{S}_l} |\mathbf{R}_{m,n}|$

  $\hat{r}' = \underset{r'}{\text{argmax}} \hat{\lambda}_1(\mathbf{R}, \mathcal{S}_{r'} \cup \hat{m}) - \hat{\lambda}_1(\mathbf{R}, \mathcal{S}_{r'})$

  $\mathcal{S}_{\hat{r}} \leftarrow \mathcal{S}_{\hat{r}} \backslash \hat{m}$, $\mathcal{S}_{\hat{r}'} \leftarrow \mathcal{S}_{\hat{r}'} \cup \hat{m}$

end for

return $\mathcal{S}_1, \mathcal{S}_2, \cdots, \mathcal{S}_{N_s}$

①Initilization: initialize all sets with uniformly distributed antennas

②Greedy searching: add the antennas that maximizes the singular value

③Limit the subarray: Remove the antenna with the least contribution

④Eliminate the influence of manual initialization: check all the sets to remove the least contributor

Outline

Simulation Results

- **In the distance-aware precoding architecture, the number of RF chains can be flexibly adjusted to match the spatial DoFs**
- **The spectral efficiency can be significantly enhanced in the near-field region**

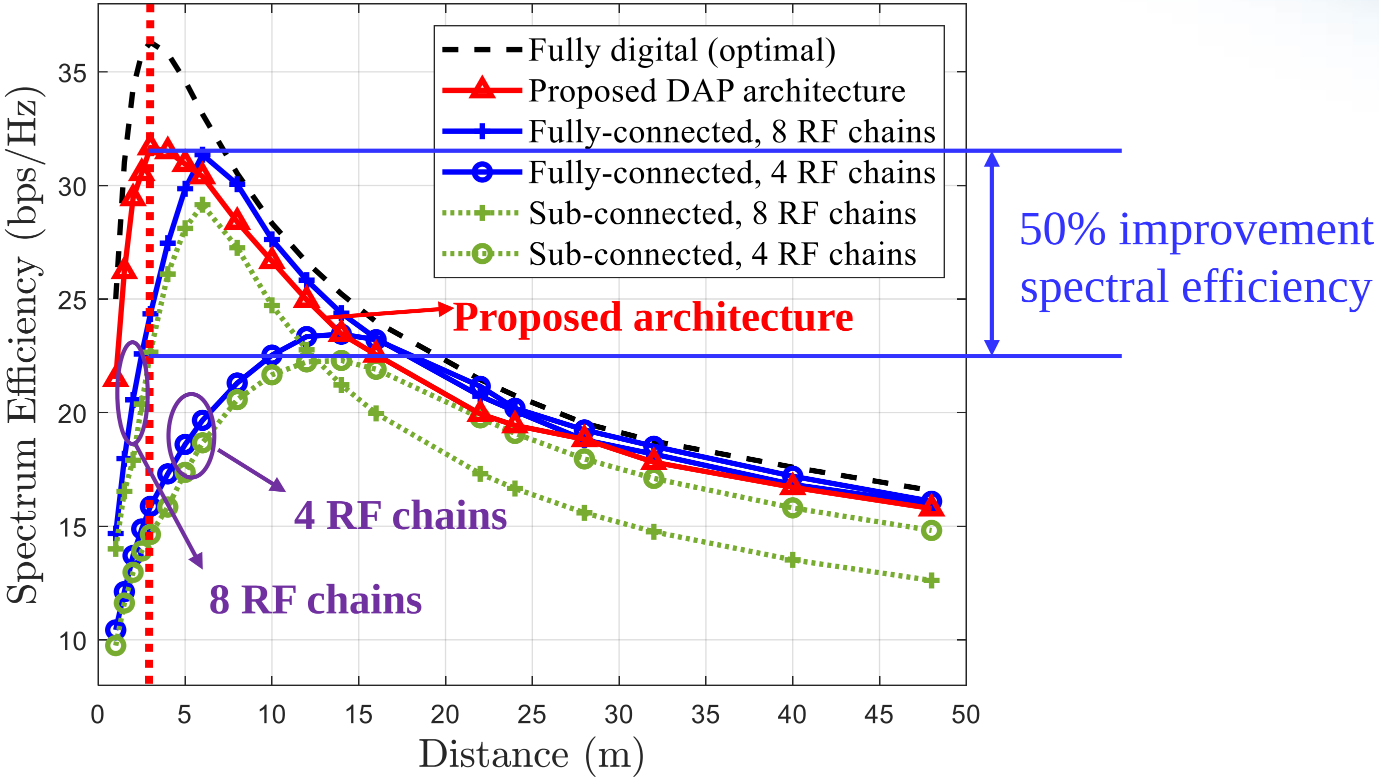

Parameters	Values
Carrier	100 GHz
BS antennas	256
MS antennas	256
SNR	30 dB

[1] X. Gao, L. Dai, S. Han, C.-L. I, and R. W. Heath, "Energy-efficient hybrid analog and digital precoding for mmwave MIMO systems with large antenna arrays," *IEEE J. Sel. Areas Commun.*, vol. 34, no. 4, pp.998–1009, Apr. 2016.

[2] X. Yu, J. Z. J. Shen, and K. B. Letaief, "Alternating minimization algorithms for hybrid precoding in millimeter wave MIMO systems," *IEEE J. Sel. Areas Commun.*, vol. 10, no. 3, pp. 485–500, Apr. 2016.

Simulation Results

- The proposed scheme also **outperforms** the existing hybrid precoding schemes in terms of **energy efficiency** in the near-field region

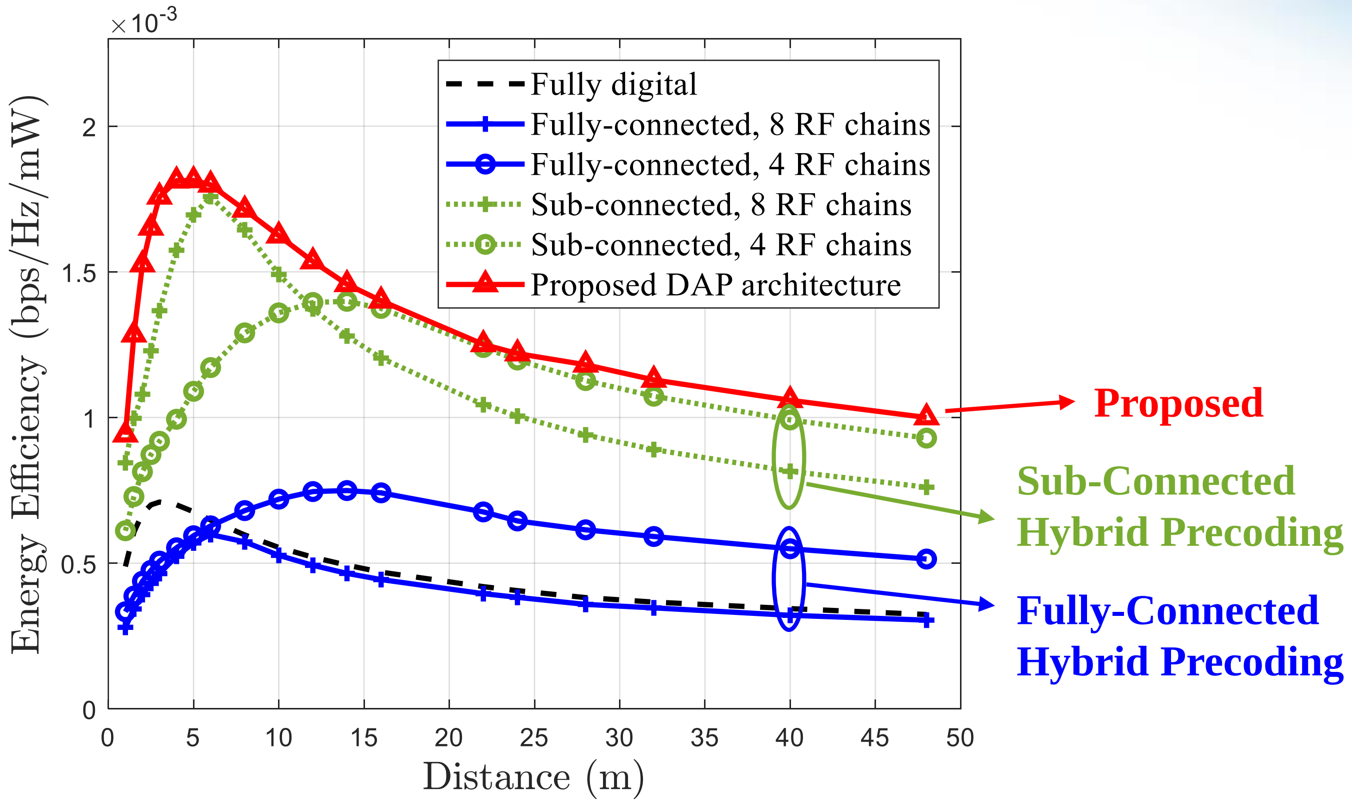

Parameters	Values
Carrier	100 GHz
BS antennas	256
MS antennas	256
SNR	30 dB

[1] X. Gao, L. Dai, S. Han, C.-L. I, and R. W. Heath, "Energy-efficient hybrid analog and digital precoding for mmwave MIMO systems with large antenna arrays," *IEEE J. Sel. Areas Commun.*, vol. 34, no. 4, pp.998–1009, Apr. 2016.

[2] X. Yu, J. Z. J. Shen, and K. B. Letaief, "Alternating minimization algorithms for hybrid precoding in millimeter wave MIMO systems," *IEEE J. Sel. Areas Commun.*, vol. 10, no. 3, pp. 485–500, Apr. 2016.

Outline

- Background
- System Model
- Proposed Precoding Architecture
- Simulation Results
- Conclusions

Conclusions

- **DoFs analysis in the near-field region**
  - **Different from the rank-one far-field LoS channel, the near-field LoS channel becomes highly-ranked**
  - **The DoFs significantly increase in the near-field region, which can enhance the channel capacity**

- **Distance-Aware Precoding (DAP) architecture**
  - **To efficiently utilize the increased DoFs in the near-field region, the DAP architecture is proposed with adjustable RF chains and selection network**
  - **Corresponding precoding algorithm is also proposed with optimized data streams N_s and selection network $\mathbf{F}_S$**
  - **Simulation results verify the superiorities on both spectral and energy efficiency**

Thank you!

Distance-Aware Precoding for Near-Field Capacity Improvement in XL-MIMO

Zidong Wu, Mingyao Cui, Zijian Zhang, and Linglong Dai

June 2022

Email: wuzd19@mails.Tsinghua.edu.cn

Website: http://oa.ee.tsinghua.edu.cn/dailinglong/